EUROFUSION WPS1-PR(16) 16210

R Reimer et al.

# Combined Zeeman and Motional Stark Effect measurements of local magnetic effects on ASDEX Upgrade

Preprint of Paper to be submitted for publication in
Nuclear Fusion

This work has been carried out within the framework of the EUROfusion Consortium and has received funding from the Euratom research and training programme 2014-2018 under grant agreement No 633053. The views and opinions expressed herein do not necessarily reflect those of the European Commission.

# Combined Zeeman and Motional Stark Effect measurements of local magnetic effects on ASDEX Upgrade

**René Reimer, Andreas Dinklage, Robert Wolf**
Max Planck Institute for Plasma Physics, 17491 Greifswald, Germany

**Oleksandr Marchuk**
Institut für Energieforschung-Plasmaphysik, Forschungszentrum Juelich GmbH, Partner in Trilateral Euregio Cluster, 52425 Jülich, Germany

**Mike Dunne, Benedikt Geiger, Jörg Hobirk, ASDEX Upgrade Team**
Max Planck Institute for Plasma Physics, 85748 Garching, Germany

**Patrick J. Mc Carthy**
Department of Physics, University College Cork, Cork, Ireland

E-mail: Andreas.Dinklage@ipp.mpg.de / Robert.Wolf@ipp.mpg.de

**Abstract.**

In view of accuracy requirements to resolve fast ion induced effects on the magnetic equilibrium, a comprehensive physics forward model is applied on the Balmer$-\alpha$ line. For the first time, the Zeeman Effect and the Motional Stark Effect (MSE) are considered in the model to analyze the spectral MSE data of a high-$\beta$ discharge with a stepwise increasing Neutral Beam Injection (NBI) heating power. The calculated magnetic field data as well as the revealed (dia)magnetic effects are consistent with the results from an equilibrium reconstruction solver. The related fast ion pressure variations derived from the spectral Zeeman and Motional Stark Effect (ZMSE) forward model data agree well within their error range with the fast ion pressure changes calculated by a transport code.

*Keywords*: Motional Stark Effect, Zeeman Effect, Zeeman-Stark Effect, Beam Emission Spectroscopy, Magnetic field measurements, Magnetically confined plasmas, Diamagnetism

## 1. Introduction

The magnetic configuration of a magnetically confined plasma is strongly related to the local plasma pressure and the current profile. The magneto-hydrodynamic force balance $\nabla p = \vec{j} \times \vec{B}$ describes a condition for stationary magnetic equilibria. Changes in the fast ion population can cause diamagnetic effects which decrease the toroidal magnetic field by about 1 % [1, 2], and these small effects, though difficult to detect, are of great importance for the local state of the plasma. Even more difficult is the measurement of changes to the local poloidal magnetic field (due to current profile reconfiguration) [3, 4, 1]. Consequently, the detection of these small variations requires highly sophisticated techniques, including corresponding qualified data analysis.
In this paper spectral Motional Stark effect measurements of the internal local magnetic field [5, 6] are performed. The concept relies on the observation of the Balmer-$\alpha$ transition ($n = 3 \rightarrow 2$) from highly energetic injected deuterium particles which are excited by collisions with ions and electrons. The beam particles have a velocity $\vec{v}_b$ with respect to the background magnetic field $\vec{B}$. For practical purposes, the emission is split into 9 observable Stark components by the electric Lorentz field, $\vec{E}_L = \vec{v}_b \times \vec{B}$, acting on atoms in their moving frame of reference. The resulting $\pi$ ($\Delta m_l = 0$) and $\sigma$ ($\Delta m_l = \pm 1$) lines of the Stark pattern are polarized parallel and perpendicular, respectively, to the local Lorentz field. Therefore, the polarization of the Stark lines is sensitive to the orientation of $\vec{E}_L$. From the line splitting, $\Delta\lambda$, the Lorentz field and thus $|\vec{B}|$ can be deduced [7, 8, 5].
In a former work [9] we found that the Zeeman effect and the fine-structure affect the line splitting by about 1 % and the intensity relation by about 3 % for a mid-sized Tokamak. Combined with the MSE it forms the so-called combined Zeeman-Stark Effect pattern [10, 11, 12, 13].
In this paper the combined Zeeman Motional Stark Effect is exploited by a forward model to measure variations in the fast ion pressure profiles in a high-$\beta$ discharge scenario. The results are consistent with results obtained from equilibrium solver (*CLISTE*) [14] and transport code (*TRANSP*) [15] calculations. Moreover, magnetic pitch angle measurements were performed and compared to *CLISTE* results.

## 2. Fast ion effects in NBI heated high-$\beta$ discharge

### *2.1. Discharge overview*

In order to asses the potential sensitivity of spectral MSE measurements to fast-ion effects, a discharge with stepwise increasing heating power up to 10.8 MW was conducted within this work. Purpose of the experiment was to examine the effect on the plasma equilibrium. Fig. 1 shows relevant time traces of discharge# 26323 on ASDEX Upgrade. Fig. 1 (a.) indicates the applied heating: Electron cyclotron heating (ECRH) was applied in order to prevent tungsten accumulation in the plasma center [16, 17, 18]. Neutral beam injection (NBI) heating with deuterium beams was provided by four 2.5 MW NBI sources for $t > 1.2$ s. The more tangentially off-axis deposited heating power of the injected NBI6, the more radially on-axis heating power of NBI8 and NBI5 are added to beam heating of NBI3 used for the sMSE diagnostic. Details about the geometry of the applied beams can be seen in Fig. 2 which shows the toroidal (a.) and poloidal view (b.) of ASDEX Upgrade. Fig. 1 (b.) indicates the total toroidal plasma current with $I_p = 0.8$ MA during the flat-

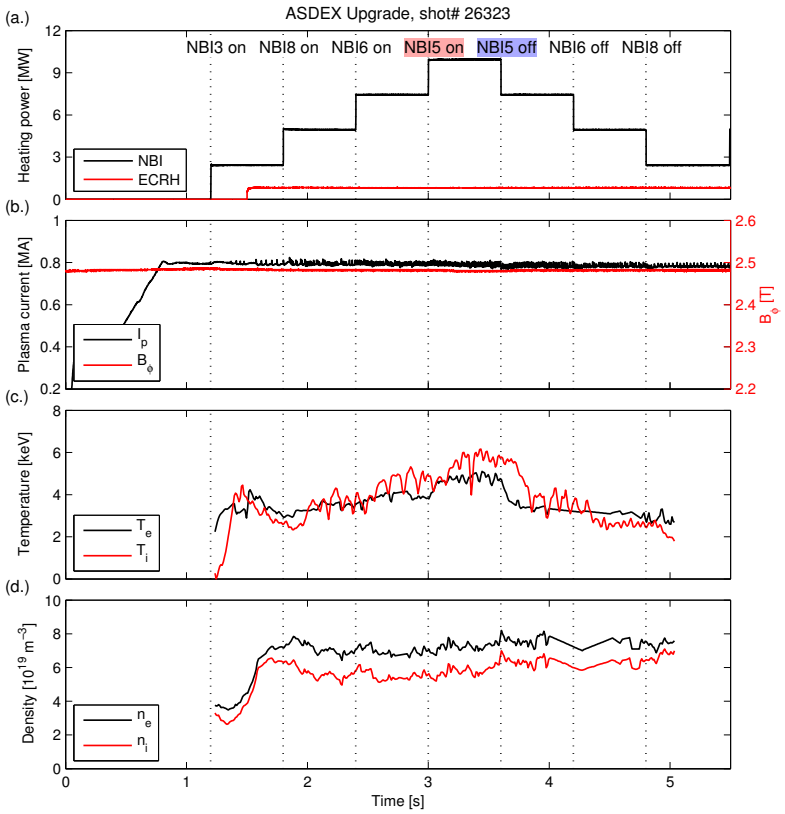


**Figure 1.** Time traces of important discharge parameters and quantities of discharge 26323 on ASDEX Upgrade: heating power (a.), plamsa current and toroidal magnetic field at axis (b.), temperature (c.) and density (d.) of ions and electrons.

top phase ($t > 0.8\,\mathrm{s}$) and the external toroidal magnetic field of $B_\phi = -2.48\,\mathrm{T}$. Fig. 1 (c.) and (d.) show the temperature and density: the black lines represent the central electron temperature ($T_e$) and central electron density ($n_e$) determined by the integrated data analysis diagnostic (IDA). The red lines indicate the central ion temperature measurements ($T_i$) from charge exchange recombination spectroscopy and the central ion density ($n_i$) resulting from $n_e$ and $Z_{eff}$ [19, 20]. The latter has a value of about $Z_{eff} \approx 1.5$. The periodic oscillations in the kinetic signals, especially in the ion and electron temperature time traces reflect the occurrence of sawtooth activity in the plasma. The main aspects of the discharge are the stepwise increase and decrease of the NBI heating power at time points indicated by the vertical dotted lines.

### *2.2. Fast ion pressure variation deduced from the forward modelled Lorentz field variation*

In this section the variation of both, total and fast ion pressure are derived from the Lorentz field as an application of the spectral combined Zeeman-Stark effect diagnostic. The results are compared to results of the equilibrium solver *CLISTE* and the transport code *TRANSP*.

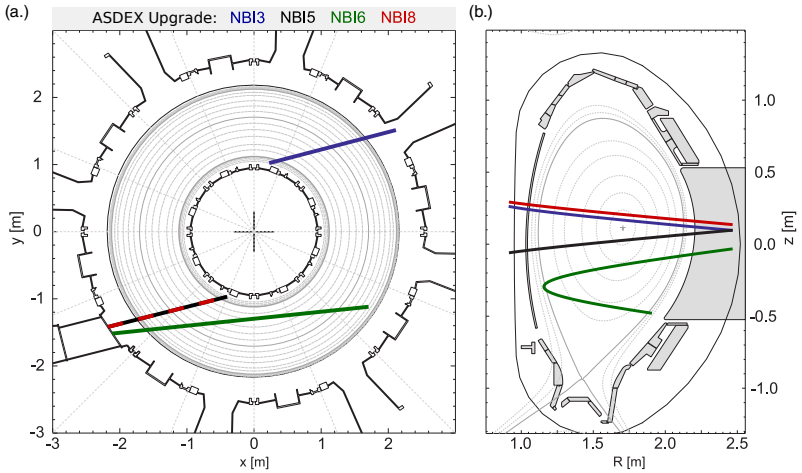


**Figure 2.** Geometry of applied neutral beam injection for discharge# 26323 - toroidal (a.) and poloidal (b.) view. Since NBI5 and NBI6 are injected from the same NBI box with the same toroidal orientation they are shown in dashed lines in the (a.).

In Fig. 3 (b.) the time traces of the central kinetic pressure, derived from the given experimental data $p_{kin} = k_B \cdot (n_e T_e + n_i T_i)$, the central fast ion pressure, $p_{FI}$, gained from the transport code *TRANSP* and the central magneto-hydrodynamic pressure, $p_{mhd} = p_{kin} + p_{FI}$, are presented. Furthermore, the stored fast ion and magneto-hydrodynamic energies, calculated with *TRANSP* are given in (b.). The corresponding time evolutions of the Lorentz fields and pitch angles calculated with the MSE forward model and the forward model of the combined Zeeman and Motional Stark effect are shown in (c.) and (d.) for a central channel.

The NBI sources differ in the direction of injection (Fig. 2 and [21]), which is of importance when discussing equilibrium results, the NBI heating sources mainly generate fast ions in the direction of heating. NBI3, NBI5 and NBI8 point more perpendicular and only NBI6 more parallel to the magnetic field. Thus there is a higher production of fast ions with perpendicular velocity, which results in an anisotropic fast ion pressure. The *TRANSP* results confirm this and show a relation for the fast ion pressure of $p_{FI,\perp}/p_{FI,\parallel} \approx 1.3$. However, the applied equilibrium solver *CLISTE* does not take into account pressure anisotropy. Thus the fast ion pressure is assumed to be isotropic for the forthcoming analysis.

The time traces of the central total pressure and central total energy reflect the heating pattern: additional NBI heating leads to a rise and reduced NBI heating leads to a decrease of these quantities. The diamagnetic decrease in the magnetic field due to the rise in the total pressure can be observed in the decrease of the modelled Lorentz field in (c.). This behaviour is mainly related to changes in the toroidal magnetic field whereas variations in the pitch angle, shown in (d.), are mainly related to changes in the poloidal field. According to the findings in [9] the Zeeman Effect does not significantly change the shape of the Lorentz field and the pitch angle but contributes as an offset in these magnetic quantities.

As depicted in Fig. 3 (b.) additional NBI heating not only increases the thermal plasma pressure but also increases the production of high energetic particles (fast

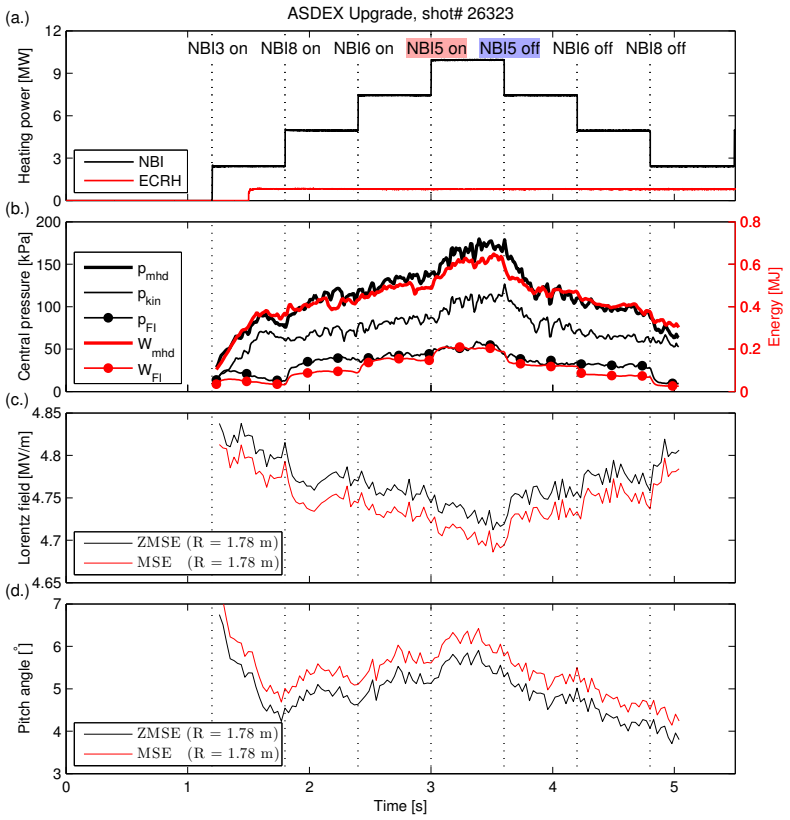


**Figure 3.** Time traces of central kinetic, mhd and fast ion pressure as well as the related stored mhd and fast ion energies (b.). The time evolution of the forward modelled Lorentz fields and pitch angles are shown in (c.) and (d.), respectively.

ions), which gyrate around their guiding center and thus induce a magnetic field component almost anti-parallel to the toroidal magnetic field. The high contribution of the fast ion pressure in the total pressure of more than 30 % indicates that the generated fast ions lead to detectable changes in the magnetic configuration and need to be considered in equilibrium reconstruction. This effect is reduced for lower total pressures.

In Fig. 4 the time evolution of the Lorentz field calculated with the improved forward model (a.) is compared to results of *CLISTE* (b.) for five different radial positions. On top of the figures the applied method is labelled. The *CLISTE* run was constrained by external magnetic measurements, the safety factor on the magnetic axis ($q_{ax} = 1$) and by the total pressure profile.

The time traces of *CLISTE* calculated signals show a significant response on the heating variation consistent to the findings for the forward modelled Lorentz fields in Fig. 3 (c.). The stepwise increase and decrease of the NBI heating power lead to a change in the measured Lorentz field followed by an exponential decay phase. As similar to findings discussed in the previous section, the ZMSE data show a lower noise level for the outer channels than *CLISTE* data. Towards the plasma core the noise level of the ZMSE data rises due to the beam attenuation. In order to calculate

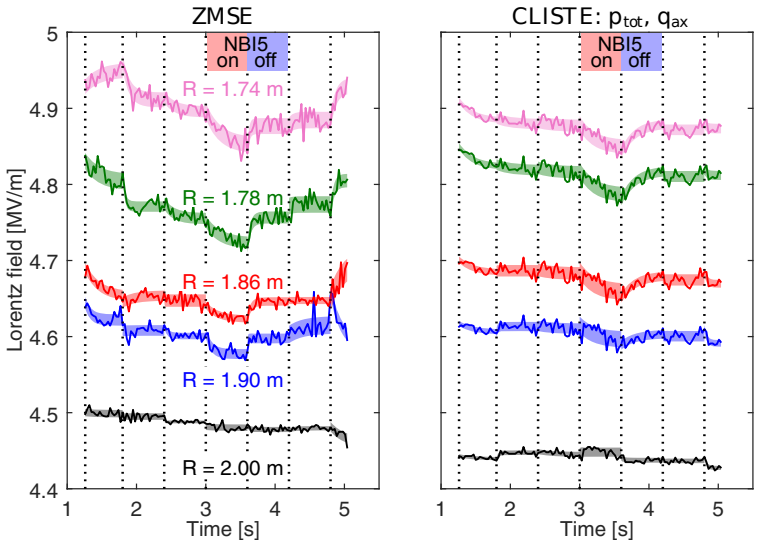


**Figure 4.** Lorentz field calculated with ZMSE Forward model (a.) and *CLISTE* right (b.). The *CLISTE* run was constrained by magnetic edge data and by a total pressure profile, $q$ was set 1 at the axis. The data were fit with an exponential approach as shown by Eq. 1. The shadowed regions indicate the $1\sigma$ error band of the fit.

the Lorentz field variation due to changes in the heating scenario the *CLISTE* and forward model data were fitted with an exponential decay:

$$E(t) = E_0 + \Delta E \left(1 - \exp\left(-\frac{t_0 - t}{\tau_D}\right)\right), \tag{1}$$

with the fit parameter $E_0$ denoting the Lorentz field at the beginning of each heating phase, $\Delta E$ denoting the amplitude of the change of the Lorentz field and $\tau_D$ the decay time. The latter fit parameter is a measure for the confinement times in ASDEX Upgrade.

The obtained values differ in a range of 20 ms ... 160 ms with a high uncertainty of about 50 ms due to the high noise and low time resolution in the data. However, these times agree in magnitude with the known slowing down times of fast ions and with the energy confinement time for the ASDEX Upgrade, which are about 60 ms. $t_0$ and represents the onset-time of each heating scenario phase. All four parameter are dependent of the heating interval and of the position $(R, z)$. The shaded area indicates the $1\sigma$ interval of confidence of the fit. The channel dependent deviation of 0.45 % (Ch1)... 1 % (Ch4) with a mean deviation of $\overline{rms} = 0.7\,\%$ indicates a good agreement between these models for this discharge. Both models show a similar response on the heating variation in the calculated Lorentz field.

From the related Lorentz field variation the total pressure variation can be deduced using the pressure balance equation in cylindrical approximation

$$\frac{dp}{dr} + \frac{B_\theta}{\mu_0 r} \cdot \frac{d\,(rB_\theta)}{dr} = j_\theta B_\phi, \tag{2}$$

with the poloidal current density

$$j_\theta = -\frac{1}{\mu_0} \cdot \frac{dB_\phi}{dr} \tag{3}$$

the magnetic permeability $\mu_0$ and the minor radius $r$. For the diamagnetic limit, where the pressure gradient is the dominating part Eq. 2 can be reduced to

$$\frac{d}{dr}\left(p + \frac{B_\phi^2}{2\mu_0}\right) = 0 \tag{4}$$

The measured Lorentz field is mainly related to the toroidal magnetic field. Thus modifications in the toroidal magnetic field can be approximated by Lorentz field variations and the pressure balance equation for the diamagnetic limit can be written as:

$$\Delta p \approx -\frac{\Delta E_L^{Dia}}{E_L} \cdot \frac{B^2}{\mu_0}, \tag{5}$$

In order to take into account only the diamagnetic effect ($\Delta E_L^{Dia}$), Lorentz field changes due to the Shafranov shift ($\Delta E_L^S$) need to be subtracted from the measured total Lorentz field variation ($\Delta E_L$). The contribution of the Shafranov shift to the total field variation is calculated by the *CLISTE* equilibrium code and is approximately given by $\Delta E_L^s / E_L \leq 0.1\,\%$.

Fig. 5 (a.) and (b.) show the variations of the pressure for the most significant cases when NBI5 is switched on (a.) and off (b.). Results from different methods *TRANSP* (mhd), kinetic measurements (kin), forward model (ZMSE) and *CLISTE* (CL) are compared with each other. Consistent with the findings in Fig. 3 (b.), additional heat load leads to a rise and reduced heating to a decrease of the total pressure and kinetic pressure. The effect of the heating is most significant in the plasma center, here $|\Delta p_{tot}| \approx 40\,\text{kPa}$ and $|\Delta p_{kin}| \approx 23\,\text{kPa}$ when NBI5 is switched on. Towards the the plasma edge the pressure variation vanishes. This indicates that the pressure profile gradient increases with additional NBI heating and *vice versa*.

The pressure profile gradient calculated from the forward model data shows the same behaviour. In fact, within the errors, the forward modelled data (black bold line) show a good agreement with the total pressure results from *TRANSP* (black dashed line) for both, NBI5 on and NBI5 off, cases. Moreover, these results are consistent with the determination of the total pressure variation by *CLISTE*. It should be noted that the *CLISTE* calculations showed low sensitivity to the pressure profile it was constrained with, which indicates that *CLISTE* is operating at its limit of sensitivity. In the error the channel and time dependent uncertainties of $\Delta E_L$, $E_L$ and of $B$ are included.

With the knowledge of the kinetic pressure change the fast ion pressure variation can be calculated. The results (black line with symbols) are compared with the *TRANSP* calculations (red dashed lines) in the panels (c.) and (d.) of Fig. 5 for the transitions NBI5 on and NBI5 off. Although there are discrepancies of about $1 \ldots 5\,\text{kPa}$ the profiles shape agrees with each other and the data fit within their $1\sigma$ confidence interval. It can be concluded that with the spectral ZMSE diagnostic small changes in the magnetic configuration and, moreover, total pressure and thus together with the kinetic pressure from kinetic measurements the fast ion pressure variations can be detected.

The measured magnetic effects and the related pressure profile variations can be expressed by the plasma $\beta$ which represents the performance of the plasma. Considering Eq. 5 the local $\beta$ is deduced from forward model data and *CLISTE* data:

$$\Delta\beta \approx -2\frac{\Delta E_L}{E_L}. \tag{6}$$

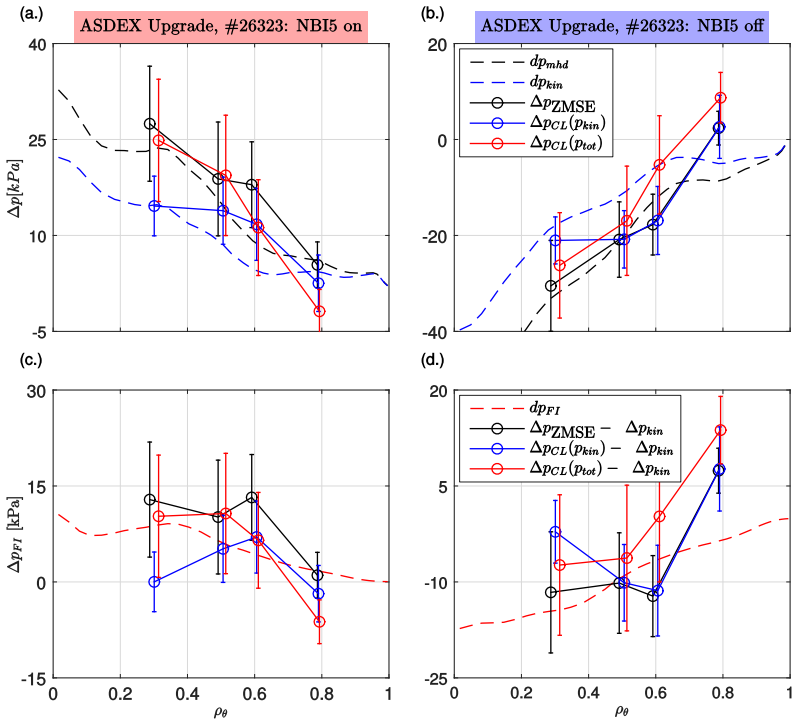


**Figure 5.** Comparison of pressure profile variations for the heating scenario transition NBI5 switched on (a.) and (c.) and NBI5 switched off (b.) and (d.): the upper panels show the total and kinetic pressure variation, the lower pannels present fast ion pressure variation. Error bars from error propagation equation taking into account the $1\sigma$ uncertainty of $\Delta E_L$, $E_L$ and $B$.

In Fig. 6 the local $\beta$ variation calculated with the forward model and with *CLISTE* is shown for the cases NBI5 on (a.) and NBI5 off (b.). It can be seen that with increasing heating the plasma leads to an increase of the local and global plasma $\beta$ (a.). The effect is up to $\approx 1\,\%$ in the plasma center and vanishes towards the outer region. The local increase is consistent with the observed local diamagnetic effect due to the rise of the local total pressure. Switching off the heating source NBI5 has the opposite effect. The decreased total plasma pressure and increased magnetic field leads to a lower plasma confinement (b.). The agreement between equilibrium reconstruction data and the forward model data demonstrates the potential of the spectral ZMSE diagnostic to detect both, the total pressure variations and the related diamagnetic effects.

### *2.3. Pitch angle*

As shown in [22] the MSE forward model allows the evaluation of the pitch angle from the ratio of the $\sigma$ and $\pi$ lines from the MSE spectrum [21, 22]. This is still valid for the extended model. Two other methods determining the pitch angle independently are the MSE polarimetry, which applies the central $\sigma_0$ line from the MSE spectrum and the equilibrium reconstruction by solving the Grad-Shafranov equation. In Fig. 7 the time traces of the forward modelled pitch angles (b.) are compared with time

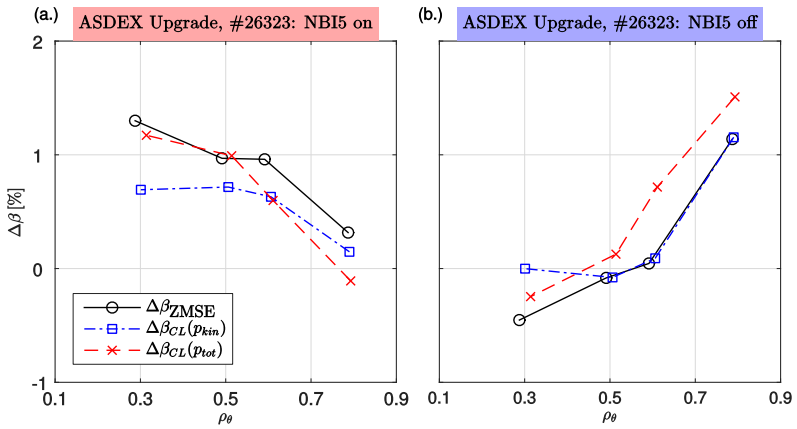


**Figure 6.** Variation of the local plasma $\beta$ for the heating scenario transition NBI5 switched on (a.) and NBI5 switched off (b.). Forward model data are compared to two diferent *CLISTE* run data.

traces calculated by the equilibrium solver *CLISTE* (a.) and MSE polarimetry (c.). All three methods are able to detect variations in the pitch angles due to changes in the plasma heating. Increasing NBI heating leads to a rise of the pitch angles and vice versa, except for the outer channels. Consistently to the results from Sec. 2.2 the effect is most significant in the center. The statistical noise is indicated with a shaded area. The remarkable low noise-level of the forward modelled data is about $0.12\,^\circ$ (Ch1)...$0.21^\circ$ (Ch4) which is about 30 % of the MSE polarimetry noise-level. Similar to the Lorentz field data the beam attenuation lead to a high uncertainty in the Forward modelled pitch angle for the central channel and are not useful for the later analysis. An offset correction was necessary to bring the data at the same level. The correction has been performed by a minimizing model, that minimizes the difference $\epsilon_i$ between *CLISTE* and Forward model and *CLISTE* and MSE polarimetry data: $\epsilon_1 = d_{CLISTE} - d_{ZMSE}$ and $\epsilon_2 = d_{CLISTE} - d_{MSEp}$. The channel dependent bias is given for each channel in the gray boxes in Fig. 7. As can be seen for this discharge, the offsets of both MSE diagnostics differ channel dependent within the range of $0.4^\circ$. The effects responsible for the offsets are not yet fully understood, but are matter of current investigation [5, 23]. First results indicate that besides such apparatus effects as coating on the vacuum window, or ageing of the photo elastic modulators of the polarimeter set-up, reflection in the plasma vessel is a likely cause. The offset of the spectral diagnostic is $\gamma_0(\mathrm{ZMSE}) = \gamma_0(\mathrm{ZMSE}) - 0.5\,^\circ$. Due to the occurrence of the offset in the pitch angle the full potential of the spectral MSE diagnostic, the self-consistent calculation of the magnetic field, could not could not be applied. However, besides the calculation of absolute values of $E_L$, the diagnostic can be applied to measure variations in the pitch angle, e.g. due to changes in the heating scenario.
All three methods, the equilibrium code *CLISTE*, the forward model and the MSE polarimetry diagnostic, showed the most significant changes in $\gamma$ when NBI source 5 was switched on and after it was switched off again, cf. Fig. 7. In Fig. 8 the profiles of the pitch angle variation, calculated with the three methods, are presented for both, the NBI5 on transition phase (a.) and the NBI5 off transition phase (b.). It can be seen that for the first case $\gamma$ decreases at the outer channels but rises at the inner channels. This is vice versa, for the second case, where NBI5 is switched

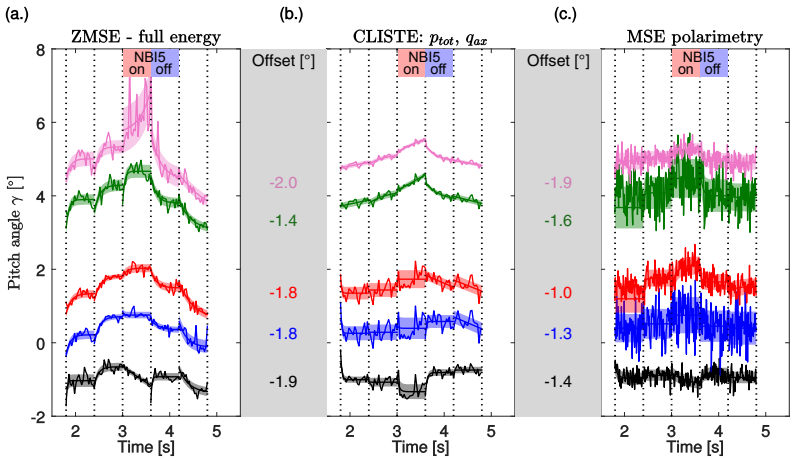


**Figure 7.** $\gamma$-comparison between forward model (a.), *CLISTE* (b.) and MSE polarimetry (c.) results. Forward model and MSE polarimetry results are corrected by an channel dependent offset. The offsets of both MSE diagnostics are given in the gray boxes for each channel. The shadowed regions indicate the $1\sigma$ error band.

off. Although the observed changes are small ($-0.5° \ldots 0.5°$), all the independent methods produced similar results. These facts and the aforementioned low noise level show that the spectral MSE results are trustworthy and demonstrates that the spectral MSE diagnostic fulfils required accuracies for fusion devices of about $0.1° \ldots 0.5°$ [1].

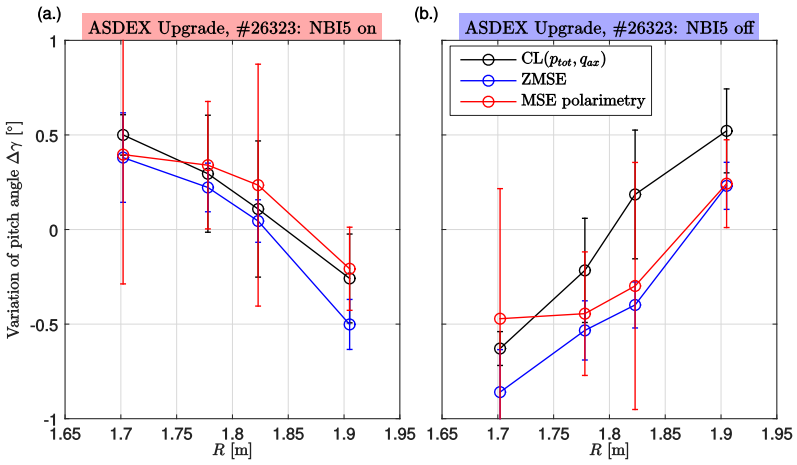


**Figure 8.** Variation of $\gamma$ due to variation in NBI heating: (a.) NBI5 switched on and (b.) NBI5 switched off. Forward model data are compared to *CLISTE* and MSE results.

## 3. Summary and Outlook

By employing the combined Zeeman Motional Stark effect on the hydrogenic heating beams a high resolution technique for the detection of small effects in the local

magnetic configuration has been developed on ASDEX Upgrade.
A ZMSE forward model, as described in **??**, was applied to determine fast ion variations in a high-$\beta$ discharge scenario with stepwise increasing and decreasing NBI heating power. The rise of the fast ion pressure with additional NBI heating power could be determined from their measured local diamagnetic effect observed in the Lorentz field. The changes of the fast ion pressure of $\approx 0\,\mathrm{kPa}$ at the plasma edge to $15\,\mathrm{kPa}$ at the plasma center are consistent with results from *TRANSP* and *CLISTE*. The improved plasma confinement $\beta$ also derived from the Lorentz field variation agrees with predictions from the *CLISTE*. A reduction in the heating power lead to a reduction of the diamagnetic effect in the plasma. The fast ion pressure as well as the local $\beta$ were decreased.
Effects of the fast ions in the pitch angle could be seen in the time development of $\gamma$ and were compared to equilibrium reconstruction results of *CLISTE* and to MSE polarimetry data. The channel dependent precision of about $0.12^\circ \ldots 0.21^\circ$ is about $30\,\%$ of the precision of the data of the MSE polarimetry. The observed channel dependent deviation of around $-1^\circ \ldots -1.5^\circ$ between ZMSE and *CLISTE* data are consistent with the offset which was also observed by the ASDEX Upgrade MSE polarimetry diagnostic. Once the offset can be determined by a physical model, the full potential of the spectral ZMSE diagnostic, a self consistent reconstruction of the magnetic field, can be exploited. Good agreement between *CLISTE* and forward model data were found for the pitch angle variation for chosen discharge scenario transitions.
Further improvements could be expected by the reduction of the noise by improved hardware settings, e.g. using a less complex optical path by omitting the polarimeter set-up. Furthermore the uncertainty of the data have shown the need of a full statistical description of the forward model, for example by a bayesian approach. Moreover, the forward model can be refined by considering additional electric field components, e.g. radial electric field.

## Acknowledgement

This work has been carried out within the framework of the EUROfusion Consortium and has received funding from the Euratom research and training programme 2014-2018 under grant agreement No 633053. The views and opinions expressed herein do not necessarily reflect those of the European Commission. The authors would like to express their gratitude to the members of the Wendelstein 7-X (W7-X) and the ASDEX Upgrade for valuable discussions. A special thank goes to the ASDEX Upgrade operation team for the successful conduction of the necessary experiments.

## References

[1] Wolf R, O'Rourke J, Edwards A and von Hellermann M 993 Nucl. Fusion **33** 663–667 URL http://iopscience.iop.org/article/10.1088/0029-5515/33/4/I13/pdf
[2] Wolf R 1993 Measurement of the Local Magnetic Field Inside a Tokamak Plasma (JET) by Means of the Motional Stark Effect and Analysis of the Internal Magnetic Field Structure and Dynamics Ph.D. thesis Heinrich-Heine-Universität Düsseldorf
[3] Braithwaite G, Gottardi N, Magyar G, O'Rourke J, Ryan J and Veron D 1989 Rev. Sci. Instrum. **60** 2825–2834
[4] Soltwisch H 1992 Plasma Phys. Contr. Fusion **34** 1669 URL http://iopscience.iop.org/article/10.1088/0741-3335/34/12/001/pdf

[5] Wolf R, Bock A, Ford O, Reimer R, Burckhart A, Dinklage A, Hobirk J, Howard J, Reich M and Stober J 2015 J. Instr. **10** P10008 URL http://iopscience.iop.org/article/10.1088/1748-0221/10/10/P10008/pdf

[6] Voslamber D 1995 Rev. Sci. Instrum. **66** 2892–2903

[7] Foley E, Levinton F, Yuh H and Zakharov L 2008 Rev. Sci. Instrum. **79** 10F521 URL http://dx.doi.org/10.1063/1.2957776

[8] Zakharov L, Lewandowski J, Foley E, Levinton F, Yuh H, Drozdov V and McDonald D 2008 Plasma Phys. **15** URL http://dx.doi.org/10.1063/1.2977480

[9] Reimer R, Dinklage A, Dunne M, Geiger B, Hobirk J, Marchuk O, Mc Carthy P, Wolf R and ASDEX Upgrade Team and W7-X Team 2016 Plasma Phys. Contr. Fusion Submitted

[10] Isler R 1976 Phys. Rev. A **14**(3) 1015–1019 URL http://dx.doi.org/10.1103/PhysRevA.14.1015

[11] Breton C, Demichelis C, Finkenthal M and Mattioli M 1980 J. Phys. A **13** 1703–1718 URL http://iopscience.iop.org/article/10.1088/0022-3700/13/8/022/pdf

[12] Souw E and Uhlenbusch J 1983 Physica **122C** 353–374 URL http://dx.doi.org/10.1016/0378-4363(83)90063-3

[13] Mandl W 1991 Development of active Balmer-alpha spectroscopy at JET Ph.D. thesis Technische Universität München

[14] Mc Carthy P and ASDEX Upgrade Team 2012 Plasma Phys. Contr. Fusion **54** 015010 URL http://iopscience.iop.org/article/10.1088/0741-3335/54/1/015010/pdf

[15] Pankin A, Bateman G, Budny R, Kritz A, McCune D, Polevoi A and Voitsekhovitch I 2004 Comput. Phys. Commun. **164** 421–427 URL http://www.sciencedirect.com/science/article/pii/S0010465504003133

[16] Neu R, Bobkov V, Dux R, Kallenbach A, Pütterich T, Greuner H, Gruber O, Herrmann A, Hopf C, Krieger K et al. 2007 J. Nucl. Mater. **363** 52–59

[17] Wagner D, Stober J, Leuterer F, Sips G, Grünwald G, Monaco F, Munich M J, Poli E, Schütz H, Volpe F et al. 2009 IEEE Trans. Plasma Sci. **37** 395–402

[18] Hohnle H, Kasparek W, Stober J, Herrmann A, Leuterer F, Monaco F, Neu R, Schmid-Lorch D, Schutz H, Schweinzer J et al. 2010 Extension of the ecrh operational space with o2 and x3 heating schemes to control w accumulation in asdex upgrade Tech. rep. ASDEX Upgrade Team

[19] Meister H, Fischer R, Horton L, Maggi C, Nishijima D, ASDEX Upgrade Team, Giroud C, Zastrow K D, JET-EFDA Contributors and Zaniol B 2004 Rev. Sci. Instrum. **75** 4097–4099

[20] Rathgeber S, Fischer R, Fietz S, Hobirk J, Kallenbach A, Meister H, Pütterich T, Ryter F, Tardini G, Wolfrum E and ASDEX Upgrade Team 2010 Plasma Phys. Contr. Fusion **52** 095008 URL http://iopscience.iop.org/article/10.1088/0741-3335/52/9/095008/pdf

[21] Reimer R, Dinklage A, Fischer R, Hobirk J, Löbhard T, Mlynek A, Reich M, Sawyer L, Wolf R and ASDEX Upgrade Team 2013 Rev. Sci. Instrum. **84** URL http://dx.doi.org/10.1063/1.873630

[22] Dinklage A, Reimer R, Wolf R, Team W X, Reich M and ASDEX Upgrade Team 2011 Fusion Sci. Technol. **59** 406–417 URL http://epubs.ans.org/download/?a=11655

[23] Löbhard T 2011 Calibration method for the motional Stark effect diagnostic on fusion experiment ASDEX Upgrade Master's thesis Technical University of Munich